ORGANIC PROCESS RESEARCH & DEVELOPMENT
OPR&D

pubs.acs.org/OPRD

Article

Solid Form Selection and Process Development of KO-947 Drug Substances

Bo Mei, Linrong Zhu, Yushen Guo, Tao Wu, Pingda Ren, and Xiaohu Deng*

Cite This: https://doi.org/10.1021/acs.oprd.1c00113

Read Online

ACCESS | Metrics & More | Article Recommendations

ABSTRACT: KO-947 is a potent, selective extracellular signal-regulated kinases (ERK) inhibitor that was investigated in the clinic for the treatment of various solid tumors. KO-947 free base, form E, was originally recommended out of 10 identified crystalline forms for the development of an oral solid dosage product. Change of clinical need shifted the focus to aqueous solubility enhancement through salt formation. Mesylate salt demonstrated remarkably increased aqueous solubility and also profound polymorphism. Anhydrous form III was initially recommended but later dropped, primarily due to the manufacturing difficulties. In the end, form IX was discovered through close collaboration between preformulation and process scientists. An elaborate manufacturing process was then devised to successfully produce mesylate salt, form IX in kilogram scale supplied for the clinical use.

KEYWORDS: *polymorph, solubility, mesylate salt, crystallinity, hygroscopicity, stability*

INTRODUCTION

Ever since the incidence of Abbott's HIV drug Ritonavir in 1998,[1] the significant impact of solid-state form of new chemical entity (NCE) on bioavailability, stability, manufacturability, and patient compliance has been increasingly recognized by the pharmaceutical/biotechnology industry. Selection of an appropriate solid form can sometimes decide the success or failure of the discovery program, particularly for molecules exhibiting profound polymorphism. Despite considerable development of this field, it remains a substantial undertaking to balance many variables of a solid form suitable for further pharmaceutical development. Over the years, many decision paradigms have been implemented by the practitioners in the field,[2] with the common scheme of making recommendations based on physicochemical characterization of crystallinity, hygroscopicity, stability, and process control. Albeit extremely useful, a decision tree should only serve as a general guide, which has to be tailored to each molecule to meet the specific purpose.[3] To this end, whereas preformulation scientists would and should play an indispensable role, close collaboration and consultation with other functional areas such as active pharmaceutical ingredient (API) process research, formulation development, clinical, and regulatory, are critical to avoid suboptimal choices and missed opportunities. Herein, we present a case study of a holistic, integrated approach toward polymorph and salt selection for KO-947 (Figure 1). An iterative process involving inputs from many functional areas changed the course multiple times, and ultimately resulted in the selection of a mesylate salt, form IX, as the final form for the successful good manufacturing practice (GMP) API production in kilogram scale.

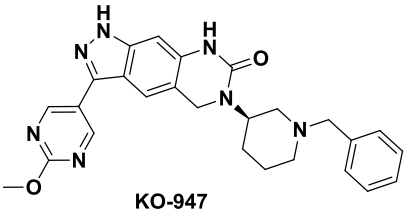

Figure 1. Chemical structure of KO-947.

RESULTS AND DISCUSSION

KO-947 is a potent, selective inhibitor discovered in our laboratory,[4] targeting extracellular signal-regulated kinases (ERK) that sit at the bottom of the MAP kinase (MAPK) pathway, one of the most important signaling cascades that control cellular proliferation and survival. Inhibition of ERK has been proposed as a potential treatment for a range of solid tumors and has been investigated in the clinics.[5] We were advancing KO-947 to a first in human (FIH) clinical trial (https://clinicaltrials.gov/ct2/show/NCT03051035), and an appropriate solid form was needed for the formulation development and clinical trial material (CTM) manufacturing.

Free Base and Polymorph Screening. KO-947 is a lipophilic weak base with $pK_a \sim 7.9$ measured by the pH metric method. The initial identified solid form A is a

Received: April 2, 2021

nonhygroscopic, crystalline solid with a sharp melting point of 163.2 °C, as shown in Table 1.

Table 1. Characterization of KO-947, Free Base, Form A[a]

form	pK_a	melting point (°C)	log *P*	log *D* (pH)	hygroscopicity (DVS, 0−80% RH)
A	7.9	163.2	1.72	1.42 (9.0); 1.7 (7.4); 0.86 (4.0); 0.46 (1.0)	0.56%

[a]DVS, dynamic vapor sorption.

Oral administration of KO-947 was originally targeted and a polymorph screening on the free base was conducted with the aim of findign a suitable form for oral solid dosage formulations. Various screening techniques such as slurry, thermal heating−cooling, solvent evaporation, antisolvent precipitation, and grinding[6] were employed and 11 forms were identified from these efforts and the X-ray powder diffraction (XRPD) patterns are shown in Figure 2. The thermal properties of these forms were then characterized with differential scanning calorimetry (DSC) and thermal gravimetric analysis (TGA) under matching conditions and the data are summarized in Table 2. Pattern B was very similar to original pattern A with only minor difference of a few additional peaks. The melting points were similar as well. It is noted that the original form A had residual solvents which might cause the minor difference. Patterns C and D were also similar on both XRPD and thermal behavior. Forms E, I, and J appeared to have better crystallinity on XRPD than forms F, G, H, and K, which were consistent with the higher melting points on the DSC data.

We quickly noticed that KO-947 free base polymorphism was highly dependent on the solvent system used in the preparation method, presumably involving formation of solvates. This observation caused considerable concern for the process chemists since different organic solvents would likely be used in the manufacturing operations such as washing, extraction, and recrystallization, potentially leading to form changes. Therefore, solubility of original form A in various organic solvents at room temperature and potential form conversion after dissolution were investigated and summarized in Table 3.

Among all of the forms identified, form E exhibited the highest melting point at 213 °C and high crystallinity, as shown in Figure 3. The peak at 84 °C is likely from the residual solvents. A sample of form E was heated at >100 °C to remove the presumptive residual solvents and the crystalline pattern remained the same based on XRPD analysis. In addition, the solubility information (Table 3) enabled process chemists to design a robust manufacturing process to produce form E exclusively with consistent quality control.

While free base, form E, was looking promising at that time and was recommended for further characterization and scaling up, the clinical development changed course in favor of intravenous over oral administration due to potential advantages on toxicity mitigation and clinical differentiation. To develop an injectable formulation suitable for intravenous administration, water solubility became the priority in form selection.

Salt Selection. KO-947 free base is practically insoluble in water at neutral pH. Given the nature of being a weak base ($pK_a \sim 7.9$), salt formation was an obvious choice for aqueous solubility enhancement.[7] Therefore, a number of pharmaceutically acceptable acids[8] were screened from appropriate organic solvents and the isolated salts were characterized, as summarized in Table 4. Indeed, all salts investigated showed considerable aqueous solubility enhancement but mesylate (MSA) salt stood out at ∼40 mg/mL with a higher pH value of the saturated aqueous solution at ∼4.1 (form I). Although pH values of the saturated solution of forms II, III, and IV were not measured, presumably they would be comparable to form I given the similar aqueous solubility. Other properties of the salts were then investigated. All of the salts are hygroscopic

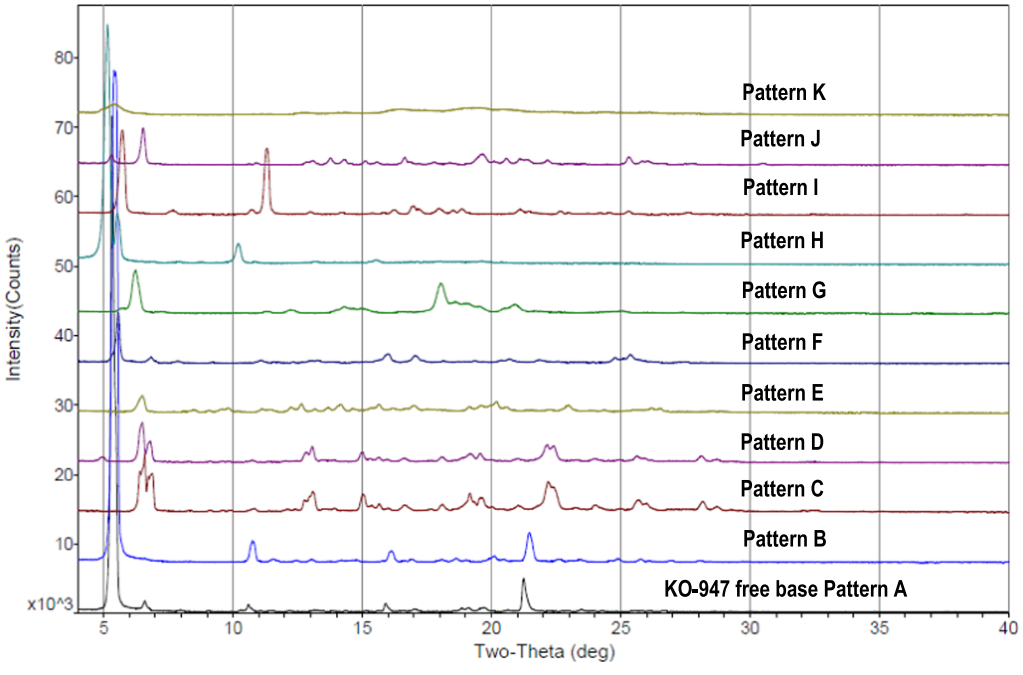

Figure 2. XRPD overlay of KO-947 free base forms.

https://doi.org/10.1021/acs.oprd.1c00113
Org. Process Res. Dev. XXXX, XXX, XXX−XXX

Table 2. Summary of Polymorphic Forms of KO-947 Free Base[aw]

form	description	preparation method	DSC peaks (endo, onset) °C/ΔH (J/g)	TGA wt % loss (temperature range)
A	original form		58.0/48.0; 163.2/41.2	6.6% (28−124 °C)[aw]
B	anhydrate	slurry in 1-butanol	158.0/27.1	0.09% (29−150 °C)
C	anhydrate	slurry in acetone	181.7/28.3; 209.6/7.2	0.5% (34−219 °C)
D	anhydrate	slurry in ACN	164.0/0.8; 177.7/15.7; 207.9/17.2	0.9% (34−216 °C)
E	anhydrate	slurry in MIBK	208.2/38.4	0.9% (34−219 °C)
F	hydrate	slurry in water	137.4/6.0	3.6% (33−131 °C)
G	solvate/hydrate	slurry in 2-MeTHF	27/82.8; 114.9/23.3	1.7% (27−66 °C); 6.0% (66−172 °C)
H	solvate/hydrate	slurry in ACN−water system	138.6/5.4	2.0% (30−180 °C)
I	hemihydrate	slurry in MeOH	168.0/27.0	1.7% (28−150 °C)
J	anhydrate	slurry in THF	133.5/0.9; 165.5/33.0	1.1% (33−193 °C)
K	amorphous	slurry in MTBE		7.2% (33−200 °C)

[aw]eight loss was due to the residual solvents.

Table 3. Approximate Solubility KO-947 Free Base in Organic/Aqueous Media and Residual Forms

entry	solvents	solubility (mg/mL)[a]	form[b]
1	MeOH	<3	I
2	EtOH	<1.5	A + B
3	IPA	<1.5	B
4	1-butanol	<1.5	B
5	ACN	3−10	D
6	acetone	7−15	C
7	MEK	>20	C
8	MIBK	10−20	E
9	EtOAc	5−10	C
10	*i*PrOAc	2−5	C
11	MTBE	<1.3	K
12	THF	>40	J
13	2-MeTHF	>20	G
14	toluene	<1.3	C
15	heptane	<1.3	A + B
16	cyclohexane	<1.3	A + B
17	1,4-dioxane	>20	E
18	water	<1.3	F
19	MeOH−H_2O (1:1)	<1.3	B
20	MeOH−H_2O (3:1)	<1.3	B
21	EtOH−H_2O (1:1)	<1.3	A + B
22	EtOH−H_2O (3:1)	<1.3	A + B
23	ACN−H_2O (1:1)	2−5	H
24	acetone−H_2O (1:2)	<1.3	F
25	IPA−H_2O (1:1)	<1.3	B

[a]Form A was used as the input material. [b]Saturated solution was prepared to determine the solubility. The undissolved solid was filtered, dried, and characterized with XRPD.

with a weight gain of 6.1−10.7% from 0 to 80% relative humidity (RH) as determined by dynamic vapor sorption (DVS) measurements. Both citrate and tartrate were amorphous solids. HCl salt, sulfate, besylate, and toylate afforded crystalline solids but lower purity (87.8, 91.1, 60.3, and 56.0%, respectively) than the input free base material (~99%). In addition, a short-term stability study at 40 °C/75% RH for 1 week showed further degradation of these four salts, indicating stability liability. Therefore, these salts were not pursued further.

Intrigued by the drastically improved intrinsic aqueous solubility of the mesylate salt, pH−solubility profile of the mesylate (form III) was further studied along with free base (form E) as the benchmark, as presented in Table 5 and Figure 4. Compared with the free base, considerable solubility enhancements were observed across all pH levels and respectable intrinsic solubilities were achieved at pH ≤ 6.0, which opened up abundant opportunities for the drug product formulation choices[9] and prompted us to explore further.

Albeit promising from these initial results, potential liabilities of the mesylate salt were quickly recognized. First, ever since the "bad smell" incident of Viracept in 2007,[10] mesylate salts in general have become somewhat a taboo in the industry because of the potential genotoxicity concern of mesylate esters such as methyl or ethyl methanesulfonate (EMS). Although this topic has been thoroughly studied,[11] the industry has generally been cautious of mesylate salts unless tight control of mesylate ester impurities can be implemented. Second, profound polymorphism has already manifested for KO-947 mesylate salt with four forms identified during the initial screen. Third, hygroscopicity (10.7% for form I) and chemical instability of KO-947 mesylate salts were obvious concerns.[12] Nevertheless, the team believed that the advantages associated with the drastically enhanced solubility outweighed these potential issues and embarked on a polymorph screening. Nine crystalline polymorphs of the mesylate salt were identified and the XRPD overlay was summarized in Figure 5.

The thermal properties of these mesylate forms were then characterized with DSC/TGA and the chemical stability was evaluated by the initial purity of the isolated solid and 1-week stability at 40 °C/75% RH. Form I is likely a hydrate with poor solid purity. Form II is a dihydrate and showed poor solid purity and was thermally unstable. Form IV was only observed from the isopropyl alcohol/tetrahydrofuran (IPA/THF) mixed solvent system during screening and had poor crystallinity and solid stability and hence was not investigated further. Forms V, VI, and VII are all metastable hydrates with various water stoichiometries and form changes were observed upon isolation or drying. In contrast, form III is highly crystalline and likely an anhydrate form that might contain some amount of surface water as indicated in the TGA/DSC (Figure 6). DSC also showed one endothermic peak with an onset at 223.7 °C and an exothermic peak with the onset at 281.0 °C. We attribute the endothermic peak to the chemical reaction between KO-947 free base and MSA and the exothermic peak to the subsequent decomposition, respectively.

Given the good aqueous solubility of mesylate and the many hydrate forms identified, water apparently plays a critical role. A series of water activity experiments in various organic/water solvent systems were then designed to understand the complex

https://doi.org/10.1021/acs.oprd.1c00113
Org. Process Res. Dev. XXXX, XXX, XXX−XXX

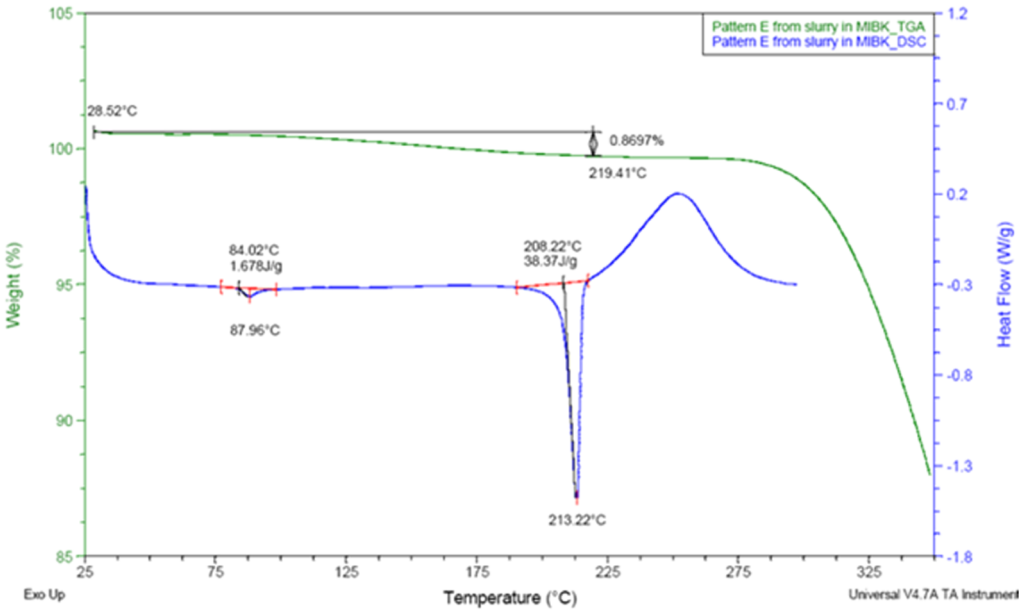

Figure 3. TGA–DSC overlay of free base, form E.

Table 4. Initial Screen of KO-947 Salts

		solubility in water					
salt[aS]	form[b]	mg/mL	pH of saturated solution	MP by DSC (°C)	DVS, % w/w (0–80% RH)	initial solid purity (%)	solid-state stability, TRS% at 40 °C/75% RH for 1 week
free base	A	<LOQ	6.5	163.2	0.5	99.0	0.0
HCl salt	I	6.4	2.8	206.3	8.9	87.8	4.9
sulfate	I	4.4	1.5	236.4	6.1	91.1	24.6
mesylate	I	40.3	4.1	205.6	10.7	95.6	4.7
	II	47.2		274.8		85.8	29.0
	III	>40		225.6	6.2	99.6	1.1
	IV	>40		280.9		88.3	31.8
besylate	I	0.54	2.0[c]	213.0	8.1	60.3	13.8
tosylate	I	0.35	2.5[c]	200.6	6.4	56.0	5.6
citrate	II	1.1	3.3	amorphous		96.3	0.5
tartrate	II	2.6	3.1	amorphous		97.5	1.0

[aS]alt stoichiometry was all 1:1. [b]Determined by XRPD. [c]Initial screening results. The low pH values might be due to the residual acids present in the salts. [d]TRS: total related substances % = all of the impurity peaks together.

Table 5. pH–Solubility Profile of Free Base vs Mesylate (MSA) Salt

	aqueous solubility at 25 °C, mg/mL	
pH	free base, form E[a]	mesylate, form III[b]
2	4.4	>100
3	3.3	>100
4	0.7	83
5	0.4	8.4
6	0.09	0.8
7	0.001	0.1
8	0	0.02
12	0	0.01

[a]Thermodynamic solubility in phosphate buffers was measured using the shake flask method. [b]Measured on Sirius-T3 using the potentiometric titration method.

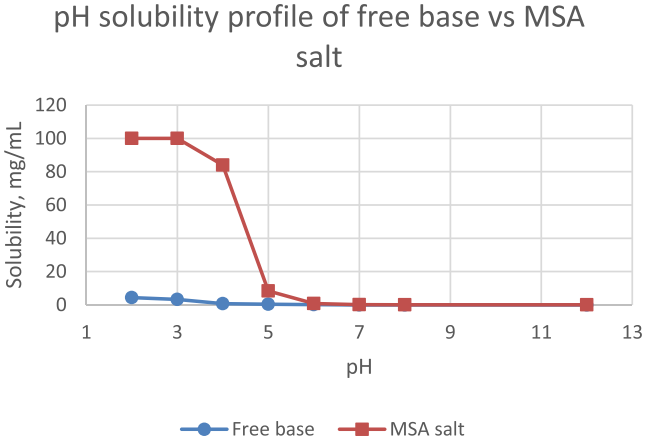

Figure 4. pH–solubility profile of free base (form E) vs mesylate salt (form III).

relationship of these forms, as summarized in Figure 7. Form II (the dihydrate form) appeared to be the predominant species

https://doi.org/10.1021/acs.oprd.1c00113
Org. Process Res. Dev. XXXX, XXX, XXX–XXX

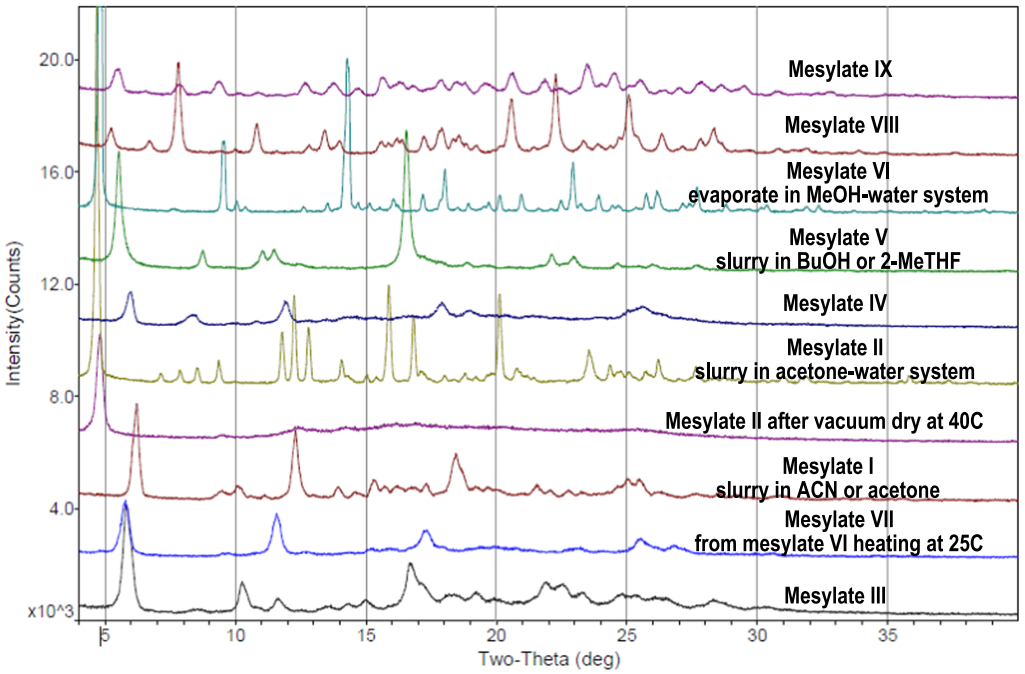

Figure 5. XRPD overlay of KO-947 mesylate salt forms.

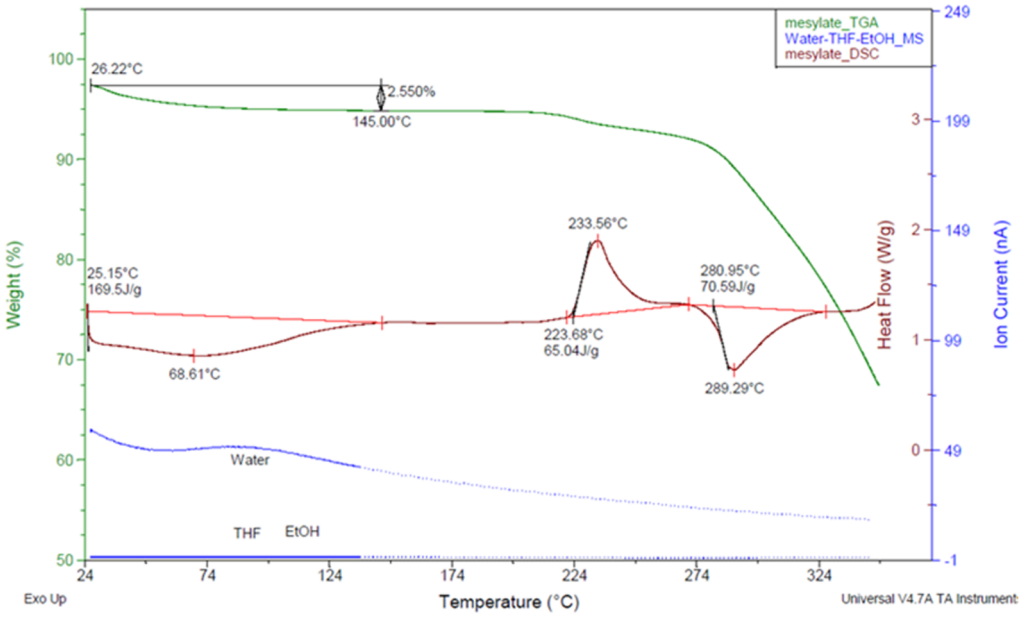

Figure 6. TGA-MS-DSC of Mesylate form III.

in the presence of water. Forms I, V, VI, and VII all converted to form II under high water activity. In addition, anhydrate form III also converted to form II when slurried in the presence of water.

Although being the most stable form in solution and highly crystalline when wet, the dihydrate form II had poor solid stability upon isolation. When being dried at 25 °C under vacuum, it completely lost the crystallinity after 3 h (Figure 8). While the crystallinity was somewhat restored upon exposure to moisture at 40 °C/75% RH, considerable amount of amorphism was observed. In combination with the chemical instability observed upon storage (Table 6), form II was not pursued further.

This left us with anhydrate form III, which had many favorable properties such as high aqueous solubility, relatively good chemical stability, moderate hygroscopicity, and high crystallinity and was recommended for further scale-up. Unfortunately, during the process development, major manufacturing issues surfaced, which proved difficult to overcome. First, form III could only be prepared in specific mixed solvent systems such as MeOH/THF or EtOH/THF. Usage of alcoholic solvents with mesylate salt, especially in the last step, raised serious concern of generating genotoxic mesylate ester impurities. Second, despite extensive optimization on crystallization processes, the particle size of form III crystal was rather small (Figure 9), which rendered substantial manufacturing difficulties in solid filtration and transfer

https://doi.org/10.1021/acs.oprd.1c00113
Org. Process Res. Dev. XXXX, XXX, XXX−XXX

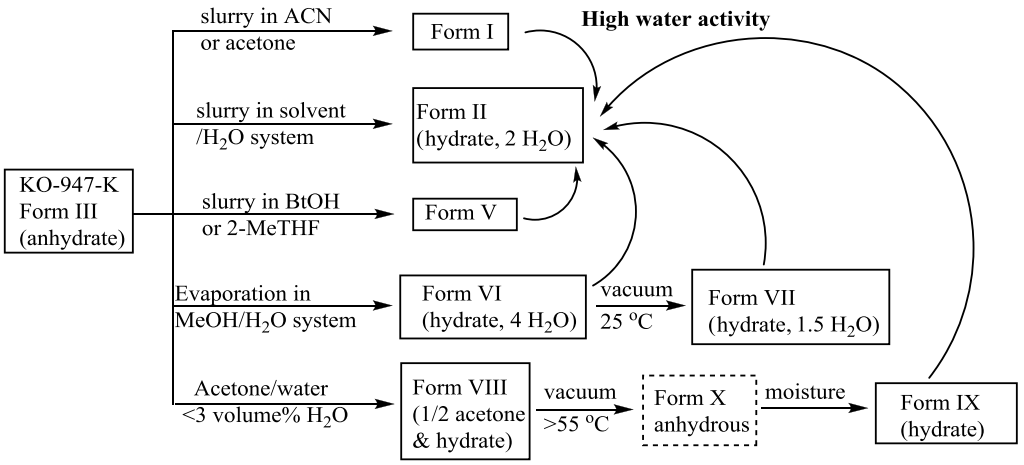

Figure 7. Relationship of KO-947 mesylate salt polymorphic forms.

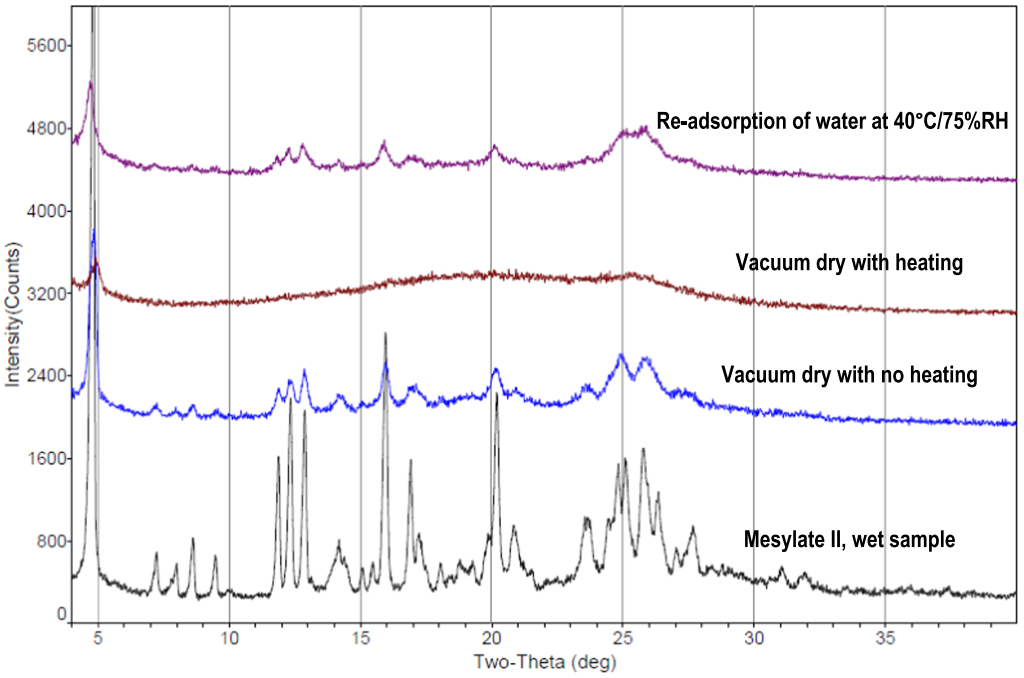

Figure 8. XRPD overlay of form II through a drying and reabsorption cycle.

Table 6. Physical Properties and Short-term Stability of the Mesylate Salt Forms

				1-week stability (TRS%)[b]	
form	description	DSC peaks, onset (°C)/exotherm−endotherm	TGA (wt % loss)	initial	40 °C/75% RH
I	hydrate	25 (endo), 206 (exo)	5.6	4.4	4.7
II	dihydrate	25 (endo), 275 (endo)	8.0	14.2	29.0
III	anhydrate	25 (endo), 224 (exo), 281(endo)	2.6	0.4	1.1
IV		25 (endo), 281 (endo)	7.1	11.7	31.8
V	metastable hydrate	73 (endo), 109 (endo), 202 (exo), 281(endo)	9.2		
VI	hydrate	54 (endo), 196 (exo)	13.3	1.0	
VII	hydrate	25 (endo), 200 (exo), 289 (endo)	5.8	4.1	
VIII	solvate/hydrate	25 (endo), 232 (exo), 285 (endo)	7.3	0.6	2.5
IX	hydrate	25 (endo), 230 (exo), 282 (endo)	3.6	0.5	1.0

[a]In addition to TGA, water loss was also confirmed with Karl Fischer measurements. [b]TRS: total related substances % = all of the impurity peaks together.

operations. Furthermore, likely related to the small particle size, the residual solvent levels were exceedingly high even after drying at elevated temperature for extended time, which exacerbated concerns on formation of genotoxic mesylate ester impurities. Therefore, mostly due to poor process feasibility, form III did not advance further.

https://doi.org/10.1021/acs.oprd.1c00113
Org. Process Res. Dev. XXXX, XXX, XXX−XXX

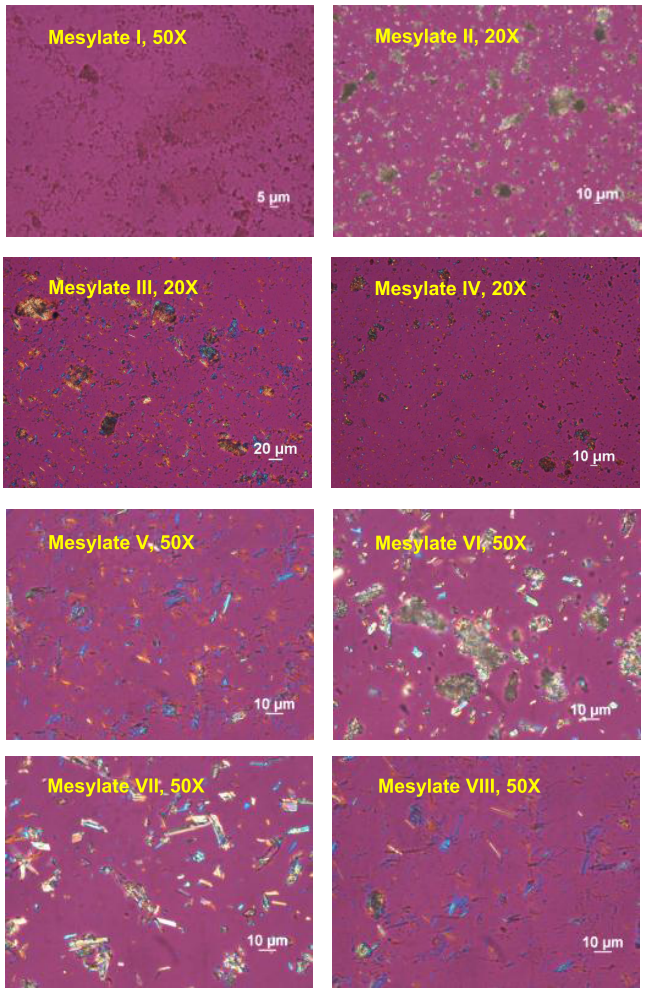

Figure 9. Polarized light microscopy (PLM) images of mesylate forms.

The team was then at an impasse and a serendipitous discovery was made. Our prior water activity studies had shown that in the presence of water, form II was the dominant species. To avoid formation of form II, the process chemists were attempting to prepare form III from anhydrous acetone but without success. Instead, a poorly crystalline salt was obtained. We reasoned that small amount of water might facilitate formation of form III, while avoiding generation of form II. To test the idea, a series of mixed acetone/water solvent systems were tried. Surprisingly, a new form that was designated as form VIII was generated exclusively when volumetric water content in the system was less than 3%. TGA/DSC (Figure 10) and ^{1}HNMR analysis revealed that form VIII was a hydrate-solvate form containing 1/2 molecule of acetone and water. Whereas form VIII possesses many favorable solid properties such as high crystallinity, desirable crystal morphology/size (Figure 9), and good chemical stability, the presence of acetone (~5.8 wt %) albeit relatively nontoxic, raises concerns clinically.

Removal of acetone from form VIII proved to be rather difficult and micronization to reduce the crystal particle size was necessary. Heating of the micronized powder at 60−70 °C under vacuum resulted in a concurrent loss of acetone and water to generate a new anhydrous form X (Figures 7 and 13). This metastable anhydrous form X was highly hygroscopic that readily absorbed water from the environment to generate another new form IX. TGA/DSC of form IX (Figure 11) showed loss of water at rather low temperature (onset 26 °C). The amount of water that form IX contained was dependent on the preparation conditions, particularly the relative humidity of the environment. The DVS study (Figure 12) showed that form IX conversion to X and back to IX was a reversible event dependent on the relative humidity. In the range of 2−65% relative humidity, the water level of form IX remained relatively stable at ~5 to 7 wt %, presumably reaching the saturated equilibrium state. The water amount was further confirmed with Karl Fischer analysis.

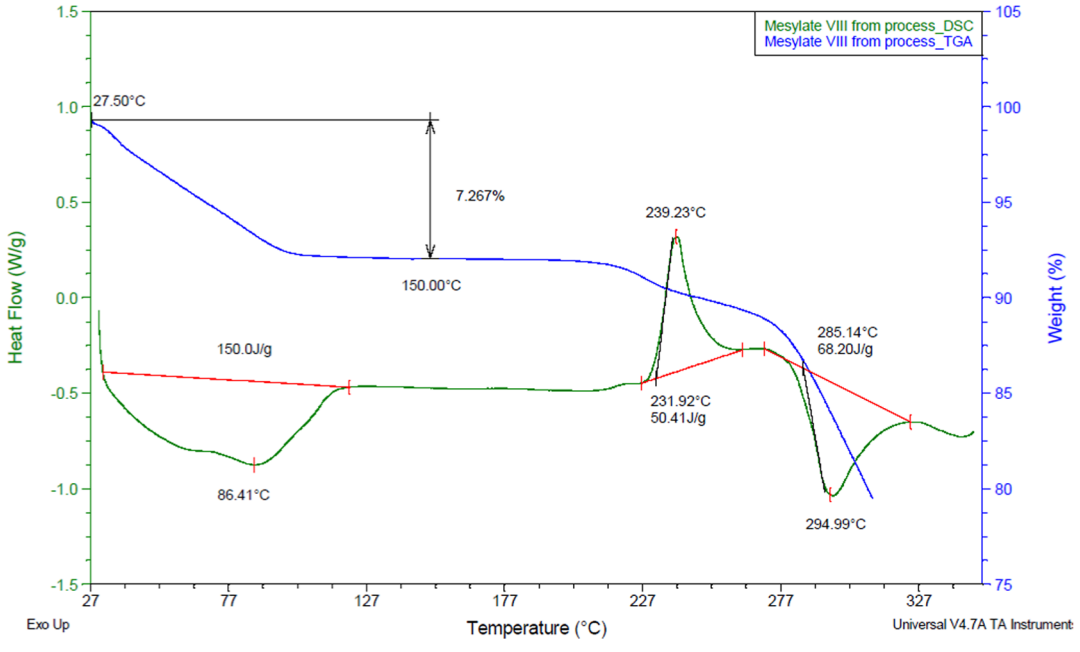

Figure 10. TGA−DSC overlay of mesylate salt form VIII.

https://doi.org/10.1021/acs.oprd.1c00113
Org. Process Res. Dev. XXXX, XXX, XXX−XXX

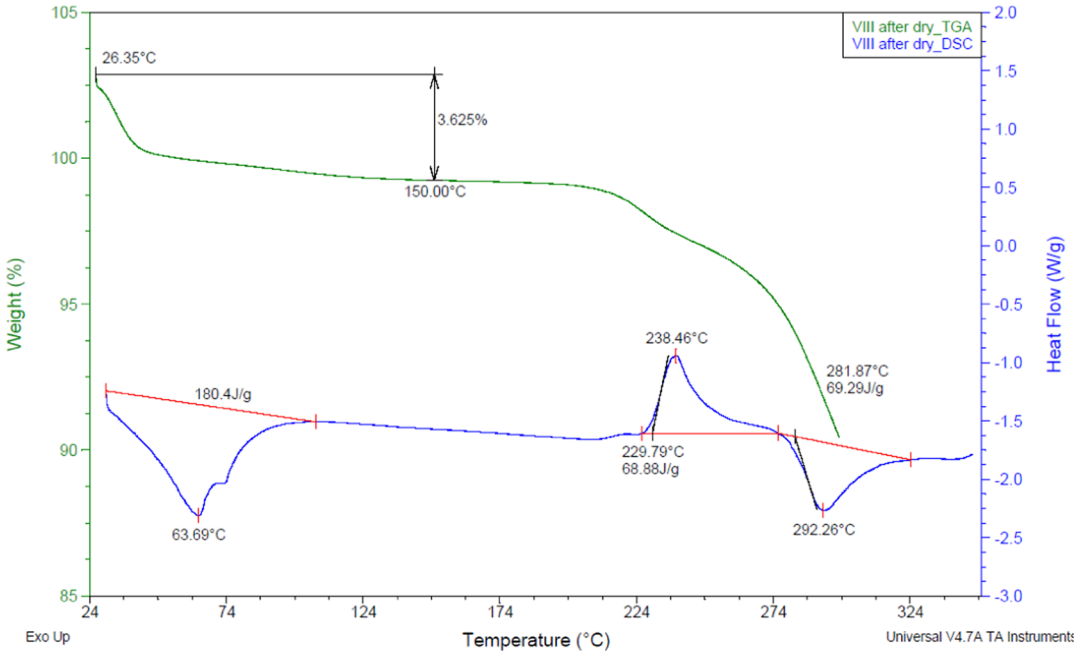

Figure 11. TGA−DSC overlay of mesylate salt form IX.

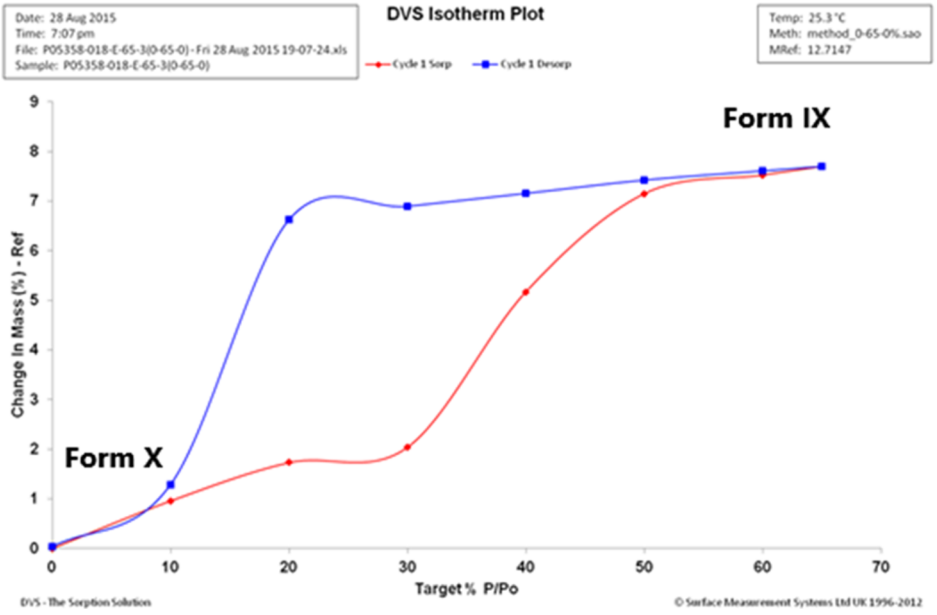

Figure 12. DVS study of mesylate salt form IX at 0−65−0% relative humidity.

The potential crystallinity change of this peculiar reversible absorption−desorption of water between forms IX and X was studied with variable temperature XRPD (Figure 13). Form IX was subjected to increasing temperatures at 30−130 °C with 10 °C increment and 10 min hold at each temperature point. Water loss of form IX occurred at >50 °C to generate the metastable form X, which was stable up to 130 °C. When form X was cooled down to 25 °C, reabsorption of water occurred to regenerate form IX. It is important to note that during the process, the crystallinity remained unchanged and no chemical degradation was observed either.

To further understand the water adsorption rate and facilitate the API manufacturing, the metastable form X, in situ generated from form IX, was exposed to various relative humidities. The time to reach equilibrium and the final weight gain were recorded on the DVS apparatus. As shown in Table 7, the water sorption rates were rather fast and constant water gain (5−7% w/w) was reached with RH > 40%, which is consistent with the previous DVS study (Figure 11).

With the above information, form IX appeared to be a viable choice to move forward. Close examination of prior screening studies showed no presence of form IX. Attempts to prepare form IX directly without going through the VIII → X → IX process in many solvent systems were not successful, as summarized in Table 8. Seeding of form IX did not help either. Not surprisingly, either form III (anhydrous conditions) or form II (high water activity) was the dominant species, which was consistent with our prior findings. We speculate that the

https://doi.org/10.1021/acs.oprd.1c00113
Org. Process Res. Dev. XXXX, XXX, XXX−XXX

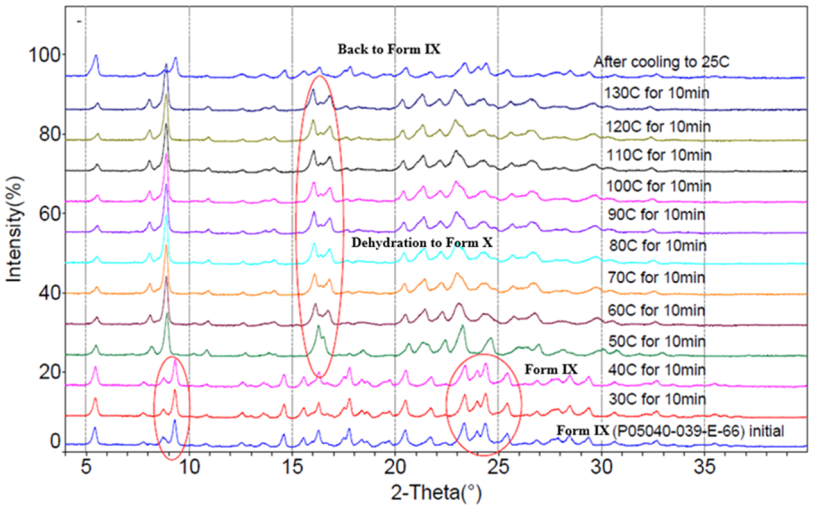

Figure 13. Variable temperature XRPD study on mesylate salt form IX.

Table 7. DVS Study on the Water Absorption Rate of Form X

condition	equilibration time (min)	weight increment (%)
30% RH	10−20	2.0
40% RH	10−20	5.5
50% RH	30−40	7.0
60% RH	20−30	7.5

Table 8. Solubility and Slurry Crystallization Study With Mesylate Salt Form III

no.	solvents	solubility (mg/mL)	XRPD pattern (dried filtered solid)
1	MeOH	10−25	III
2	EtOH	1−5	II
3	IPA	<1	III
4	1-butanol	<1	V
5	ACN	<1	I
6	acetone	<1	amorphous + I
7	MEK	<1	III
8	MIBK	<1	III
9	EtOAc	<1	III
10	*i*PrOAc	<1	III
11	MTBE	<1	III
12	THF	<1	amorphous + III
13	2-MeTHF	<1	V
14	toluene	<1	III
15	heptane	<1	III
16	cyclohexane	<1	III
17	1,4-dioxane	<1	V + III
18	water	25−50	II
19	MeOH−H_2O (1:1)	>100	II
20	MeOH−H_2O (3:1)	>100	II
21	EtOH−H_2O (1:1)	50−100	II
22	EtOH−H_2O (3:1)	>100	II
23	ACN−H_2O (1:1)	>100	II
24	acetone−H_2O (1:2)	50−100	II
25	acetone−H_2O (98:2)	<1	VIII
26	IPA−H_2O (1:1)	50−100	II

1/2 molecule of acetone was part of the crystal lattice of form VIII. Upon removal of the acetone molecule, the crystal lattice remained intact and water filled in the void to generate form IX. Therefore, direct formation of form IX without assistance of acetone might not be feasible. The similarity of DSC patterns at higher temperature region (>120 °C) for forms III (Figure 6), VIII (Figure 10), and IX (Figure 11) appears to support this hypothesis.

In the end, we settled on the following process (Figure 14) that consisted of (a) preparation of form VIII from an acetone/water system; (b) micronization followed by drying to remove acetone/water to the acceptable levels; and (c) hydration under controlled relative humidity to achieve the steady water content at 5−7 wt %. The final drug substance (form IX) manufactured in this way was crystalline, non-hygroscopic between 20 and 65% RH, and stable chemically and polymorphically. Despite the somewhat complicated manufacturing process, we believed that form IX struck a good balance as the final solid form. Using this process, KO-947 mesylate form IX was successfully manufactured in kilogram scale and the material was stable for >3 years under appropriate storage conditions. Its superb aqueous solubility enabled fast development of an injectable formulation, which was successfully used in the clinical studies.[9]

CONCLUSIONS

Drug development is a complicated process demanding collaborative efforts from the relevant functional areas. Initial polymorph screening identified free base, form E, as a favorable form for oral solid dosage products. Change of clinical need rendered solubility enhancement imperative. Mesylate salt stood out from the salt screening efforts for its dramatically increased aqueous solubility. However, mesylate salt exhibited profound polymorphic behavior. Anhydrous form III was initially recommended but later abandoned, primarily due to the manufacturing process difficulties. Form IX was later discovered through close collaboration between preformulation and process scientists. In-depth understanding of the intricate interplay among forms VIII, X, and IX rendered the design of a robust, scalable process to produce form IX as the final API in kilogram scale for the clinical use. The holistic, integrated approach involving preformulation, formulation, process chemists, and clinical input ensured rapid response to changes of course and the success of KO-947 project advancing to the clinic.

https://doi.org/10.1021/acs.oprd.1c00113
Org. Process Res. Dev. XXXX, XXX, XXX−XXX

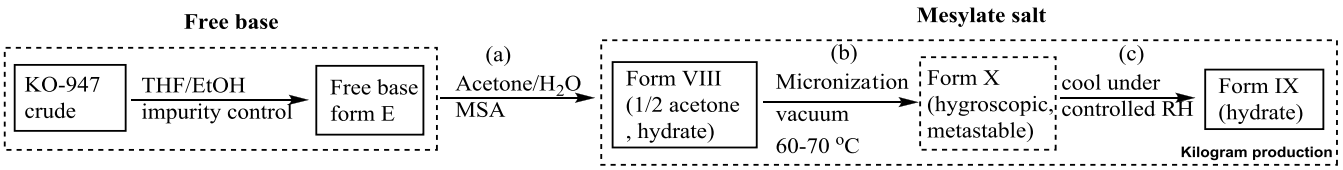

Figure 14. Robust, scalable manufacture scheme of form IX.

EXPERIMENTAL SECTION

Slurry Procedure. KO-947 free base or mesylate salt (~30 mg) suspended in appropriate amounts of solvents (Table 2 and Figures 5 and 6) was shaken at 40 °C for 24 h. The solids were dried overnight at 35 °C in a vacuum oven and then characterized by XRPD. The new forms were further characterized by DSC and TGA.

Solvent Evaporation. Free base or salts were dissolved in appropriate solvents and filtered through a 0.22 μm nylon syringe filter into clean vessels. Solvents were evaporated at 25 °C to form crystals.

Antisolvent Precipitation. Free base or salts were dissolved with good solvents at 25 °C to prepare saturated solutions, and then appropriate amounts of antisolvents were added. The precipitated solid was characterized with XRPD.

Grinding Method. Free base or salts are ground using the mortar/pestle method. The sample was pulled out after grinding for 10, 20, and 30 min and checked by XRPD.

Salt Preparation. About 100 mg of KO-947 free base was dissolved in 10 mL of solvents (acetone, THF, EtOH/THF, and IPA/THF). Acid solution predissolved in water in appropriate molar ratio was then added and the solution was stirred at room temperature. The precipitated solid was collected by filtration and characterized by PLM and XRPD.

Water Activity Study. Saturated solutions of mesylate form III in appropriate solvent systems with different water activity levels were prepared. Appropriate amounts of other forms were then added and the suspensions were slurried at 25 °C for 3−7 days. The solids were collected by centrifuge filtration and characterized by XRPD after drying.

METHODS

The PLM images were taken on a Nikon LV100 polarized light microscope (PLM). The parameters used are shown below

- Nikon LV100POL equipped with 5 MP CCD
- physical lens: 10×, 20×, and 50×

X-ray powder diffraction (XRPD) was obtained on a Bruker D8 advance diffractometer. The parameters used are shown below:

- tube: Cu Kα (λ = 1.54179 Å)
- generator: voltage: 40 kV; current: 40 mA
- scan scope: 4−40°
- sample rotation speed: 15 rpm
- scanning rate: 10°/min

Differential scanning calorimetry (DSC) was obtained on a TA Instruments Q2000 with 1−5 mg sample sealed in an aluminum pan with a pin hole on top. The method used is described below:

- heat from 30 to 300 °C (or 250 °C) at 10 °C/min

Thermal gravimetric analysis (TGA) was conducted on a TA Instruments Q5000IR equipped with MS detection. The method used is described below:

- heat from RT to 300 °C at 10 °C/min

Dynamic vapor sorption (DVS) was obtained on an SMS Advantage-1. Ten milligram samples were usually used and the parameters are described below:

- equilibrium: dm/dt: 0.01%/min (min: 10 min; max: 180 min)
- drying: 0% RH for 120 min
- RH (%) measurement step: 10%
- RH (%) measurement step scope: 0−90−0%

High-performance liquid chromatography (HPLC) analyses were used to determine solution concentration for solubility, stability, etc., which were performed on an Agilent 1260 HPLC (PDS-PF-HPLC-14) using a Water Sunfire C18, 150 mm × 4.6 mm, 3.5 μm (PDS-HPLC-082) column. Mobile phases were CAN and water with 0.05% TFA.

Production Procedure for Final Form IX. The crude KO-947 free base manufactured was dissolved in THF at 60−70 °C and EtOH was added. Seed of form E (~5%) was added and the solution was slowly cooled with agitation to room temperature. The precipitated solid was collected by filtration, washed with EtOH, and dried to afford KO-947 free base, form E.

KO-947 free base (1.0 equiv) was dissolved in a mixed solvent of acetone/water (40:1 v/v) and methanesulfonic acid (1.0 equiv) was added with stirring at 20−40 °C. The resulting suspension was stirred at 30−40 °C and then cooled to 5−15 °C. The precipitated solid was collected by filtration, washed with acetone, and dried under reduced pressure at 50−60 °C to afford mesylate form VIII (a solvate containing 1/2 acetone). The dried solid was sieved and micronized. Typical particle size distribution after micronization was D50 3.9 μm and D90 31 μm. The micronized solid was dried at 60−70 °C under vacuum to remove acetone and water to generate form X in situ and was rehydrated under a controlled relative humidity (55−65% RH) with a saturated NaBr aqueous solution until no further weight gain to afford form IX. The solid was sieved again to afford C15010401-E (KO-947-K mesylate) as an off-white solid. Typical yield is ~85% and the purity is >99%. The water content measured by Karl Fischer is 4−7 wt %.

AUTHOR INFORMATION

Corresponding Author

Xiaohu Deng − *Kura Oncology Inc, San Diego, California 92130, United States;* orcid.org/0000-0003-1393-4446; Email: xdeng1000@yahoo.com

Authors

Bo Mei − *WuXi AppTec Co., Ltd., Shanghai 200131, China*

Linrong Zhu − *WuXi AppTec Co., Ltd., Shanghai 200131, China*

Yushen Guo − *WuXi AppTec Co., Ltd., Shanghai 200131, China*

https://doi.org/10.1021/acs.oprd.1c00113
Org. Process Res. Dev. XXXX, XXX, XXX−XXX

Tao Wu − *Wellspring Biosciences Inc., San Diego, California 92121, United States*
Pingda Ren − *Kura Oncology Inc, San Diego, California 92130, United States*

Complete contact information is available at: https://pubs.acs.org/10.1021/acs.oprd.1c00113

Notes

The authors declare no competing financial interest.

■ ACKNOWLEDGMENTS

The authors thank Dr. Yi Liu and Dr. Liansheng Li for useful discussions and Dr. Tiffany Montellano and Dr. Blake Tomkinson for reviewing the manuscript.

■ REFERENCES

(1) (a) Bauer, J.; Spanton, S.; Henry, R.; Quick, J.; Dziki, W.; Porter, W.; Morris, J. Ritonavir: an extraordinary example of conformational polymorphism. *Pharm. Res.* **2001**, *18*, 859−866. (b) Morissette, S. L.; Soukasene, S.; Levinson, D.; Cima, M. J.; Almarsson, O. Elucidation of crystal form diversity of the HIV protease inhibitor Ritonavir by high-throughput crystallization. *Proc. Natl. Acad. Sci. U.S.A.* **2003**, *100*, 2180−2184.

(2) (a) *Polymorphism in Pharmaceutical Solids*; Brittain, H. G., Ed.; Marcel Dekkar: New York, 1997. (b) *Polymorphism in the Pharmaceutical Industry*; Hilfiker, R., Ed.; Wiley VCH: Weinheim, 2006.

(3) (a) Ku, M. S. Salt and polymorph selection strategy based on the biopharmaceutical classification system for early pharmaceutical development. *Am. Pharm. Rev.* **2010**, *13*, 22−30. (b) Bastin, R. J.; Bowker, M. J.; Slater, B. J. Selection and optimisation procedures for pharmaceutical new chemical entities. *Org. Process Res. Dev.* **2000**, *4*, 427−435.

(4) Li, L.; Wu, T.; Feng, J.; Ren, P.; Liu, Y. Inhibitors of ERK and Methods of Use. US Patent US9,624,228B2.

(5) Chin, H. M.; Lai, D. K.; Falchook, G. S. Extracellular signal-regulated kinase (ERK) inhibitors in oncology clinical trials. *J. Immunother. Precis. Oncol.* **2019**, *2*, 10−16.

(6) Morrison, H.; Jona, J.; Walker, S. D.; Woo, J. S. S.; Li, L.; Fang, J. Development of a suitable physical form for a sphingosine-1-phosphate receptor agonist. *Org. Process Res. Dev.* **2011**, *15*, 104−111.

(7) *Handbook of pharmaceutical salts.*; Stahl, P. H.; Wermuth, C. G., Eds.; Wiley-VCH: Weinheim, 2002.

(8) (a) Polla, G. I.; Vega, D. R.; Lanza, H.; Tombari, D. G.; Baggio, R.; Ayala, A. P.; Filho, J. M.; Fernández, D.; Leyva, G.; Dartayet, G. Thermal behaviour and stability in Olanzapine. *Int. J. Pharm.* **2005**, *301*, 33−40. (b) Reutzel-Edens, S. M.; Kleemann, R. L.; Lewellen, P. L.; Borghese, A. L.; Antoine, L. J. Crystal forms of LY334370 HCl: Isolation, solid-state characterization, and physicochemical properties. *J. Pharm. Sci.* **2003**, *92*, 1196−1205.

(9) Deng, X.; Ren, P.; Mai, W.; Wang, Y.; Zhang, Y.; Wu, H.; Xie, Y.; Chen, H. From lab formulation development to CTM manufacturing of KO-947 injectable drug products: A case study and lessons learned. *AAPS PharmSciTech* **2021**, *22*, No. 168.

(10) (a) Pozniak, A.; Müller, L.; Salgo, M.; Jones, J. K.; Larson, P.; Tweats, D. Elevated ethyl methanesulfonate (EMS) in Nelfinavir mesylate (Viracept, Roche): Overview. *AIDS Res. Ther.* **2009**, *6*, 18−23. (b) EMA report. *EMEA/CHMP/492059*; 2007.

(11) (a) Elder, D. P.; Delaney, E.; Teasdale, A.; Eyley, S.; Reif, V. D.; Jacq, K.; Facchine, K. L.; Oestrich, R. S.; Sandra, P.; David, F. The utility of sulfonate salts in drug development. *J. Pharm. Sci.* **2010**, *99*, 2948−2961. (b) Jouyban, A.; Parsa, H. Genotoxic Impurities in Pharmaceuticals. In *Toxicity and Drug Testing*; InTech Open, 2012; pp 388−414.

(12) Miller, J. M.; Collman, B. M.; Greene, L. R.; Grant, D. J. W.; Blackburn, A. C. Identifying the stable polymorph early in the drug discovery-development process. *Pharm. Dev. Technol.* **2005**, *10*, 291−297.

https://doi.org/10.1021/acs.oprd.1c00113
Org. Process Res. Dev. XXXX, XXX, XXX−XXX